

## Scaling algorithm to calculate heavy-ion spallation cross sections

C. H. Tsao,<sup>(1)</sup> R. Silberberg,<sup>(2)</sup> A. F. Barghouty,<sup>(3)</sup> L. Sihver,<sup>(4)</sup> and T. Kanai<sup>(4)</sup>

<sup>(1)</sup>*E. O. Hulburt Center for Space Research, Code 7654, Naval Research Laboratory, Washington, D.C. 20375*

<sup>(2)</sup>*Universities Space Research Association, 409 Third Street, S.W., Washington, D.C. 20024*

<sup>(3)</sup>*Physics Department, Roanoke College, Salem, Virginia 24153*

<sup>(4)</sup>*Institute of Radiological Sciences (NIRS), Chiba-shi, Inage-ku, Anagawa 4-9-1, Chiba 263, Japan*

(Received 19 November 1992)

An algorithm to scale nucleus-nucleus collision projectile-fragment cross sections from the corresponding proton-nucleus ones is developed. The algorithm takes advantage of the weak factorization property of projectile fragments. It uses the participant-spectator model and Glauber scattering theory and approximates the collision's sum rules. The algorithm is sufficiently robust over the energy range 0.1–2.0 GeV/nucleon with no restrictions on the sizes of target (apart from the special case of  ${}^4\text{He}$ ) nor projectile nuclei. It offers marked improvement over our earlier semiempirical scaling procedure. Using measured and simulated cross sections for comparison, the estimated systematic uncertainty of the algorithm averaged over this energy range is  $\sim 15\%$ .

PACS number(s): 25.70.Mn, 96.40.De

### I. INTRODUCTION

The ability to calculate with precision nuclear fragmentation cross sections is of special importance for modeling of cosmic-ray composition and propagation as most cosmic-ray nuclei with nuclear charge  $z \geq 6$  suffer nuclear collisions in the interstellar medium. These collisions alter the elemental and isotopic composition of the source. Also, the isotopes of Li, Be, and B, for example, are enhanced by several orders of magnitude as a result of nuclear spallation of heavier nuclei. In addition, flux [1] and dosimetry [2] calculations for manned space exploration, for example, are limited to a large degree by uncertainties in the nuclear spallation cross sections, especially for nuclides that have large secondary components. Some of these relevant cross sections have been measured to date, but others that are of astrophysical interest have not. Thus, procedures to predict these cross sections need to be developed.

Partial proton-induced-reaction inelastic cross sections can be estimated using the semiempirical formulas of Silberberg and Tsao [3]. Total proton-nucleus and nucleus-nucleus reaction cross sections can be estimated using the semiempirical formulas of Sihver *et al.* [4]. Heavy-ion-induced spallation cross sections can be estimated by scaling the corresponding proton-induced ones. The semiempirical scaling procedures of Letaw, Silberberg, and Tsao [5] and Silberberg and Tsao [6] tend to approximate either the low-energy behavior of the scaled cross sections or the high-energy end, but not both in a consistent fashion. Our earlier scaling procedure [4] also tends to work best for energies upward of 600 MeV nucleon. (The limitations here are primarily due to lack of data over the energy regime of interest.) The need to develop an algorithm that can approximate both behaviors then becomes clear. Moreover, reliance on salient physical properties of measured cross sections where available and simulated ones when not should guide the development of the scal-

ing procedure more so than semiempirical basis, especially when structures and energy dependence of cross sections are of special astrophysical significance.

This article describes a new scaling algorithm by which partial elemental cross sections from nucleus-nucleus collisions can be estimated by scaling the corresponding proton-nucleus cross sections. It is developed to be consistent with known empirical properties as well as conservation laws. (Some semiempirically derived [4] enhancement factors will still be used, however, for the lightest collision products.) Both data and simulation are used to test the accuracy of the algorithm and to gauge its robustness. It is intended to afford practical and CPU-efficient means by which calculated and/or experimental  $p$ -nucleus cross sections are taken advantage of to calculate the corresponding nucleus-nucleus cross sections for modeling and simulation purposes. In Sec. II, we describe the algorithm and in Sec. III, we test it for accuracy and robustness using measured and simulated data. In Sec. IV, we offer some concluding remarks after a brief summary.

### II. SCALING ALGORITHM

The procedure relies on the experimentally verified [7] concept that projectile-fragmentation cross sections obey the so-called weak factorization property. (Note that our earlier semiempirical scaling procedure [4] also took advantage of this property.) In this concept the partial cross section for the production of fragment  $f$  can be expressed as

$$\sigma_f = \Gamma_p^f \Gamma_{p,T}, \quad (1)$$

where  $\Gamma_p^f$  is a factor which depends upon the species of projectile and fragment (and as such containing the detailed dynamics), and  $\Gamma_{p,T}$  is a factor which depends only upon the species of the projectile and target. Since we

are interested in projectile fragments, in this procedure  $\Gamma_p^f$  is taken to be proportional to the predicted  $p$ -nucleus cross section for the production of the projectile fragment  $f$  (the choice to scale to proton-induced fragmentation cross sections is arbitrary and does not invalidate the weak factorization property [7] and was made solely because of the availability of the semiempirical cross-section predictions [3]), i.e.,

$$\Gamma_p^f \rightarrow \gamma_p^f = \sigma_f(\text{proj} + \text{proton} \rightarrow f). \quad (2)$$

Hence, the factorization property is now written

$$\sigma_f = \gamma_p^f \gamma_{P,T}, \quad (3)$$

where it follows from Eqs. (1)–(3) that  $\Gamma_{P,T}$  is different from but geometrically related to  $\gamma_{P,T}$ . The dimensionless factor  $\gamma_{P,T}$  is developed with the participant-spectator model [8] in mind. In collisions between nuclei at high energy (a few hundred MeV/nucleon up to few GeV/nucleon) only some (due to geometry and nuclear transparency) of the nucleons in the target and projectile nuclei actually participate in the collision dynamics (and thus the production of the various species). Those that participate are called “participants” while the others are called “spectators.” Participants from both target and projectile nuclei in the overlap geometrical volume (interaction volume) carry a considerable portion of the projectile energy which is converted into heat and high temperatures are reached. Spectator matter, in contrast, remains relatively cold even though it can be excited by the additional surface energy (typically 1 MeV fm<sup>-2</sup>) and by the few participants that have penetrated the spectator matter [8]. Estimates for projectile and target (average) participants can be written down using Glauber scattering theory [9]:

$$\langle A_{P,T}^{\text{parti}} \rangle \approx A_{P,T} \frac{A_{T,P}^{2/3}}{(A_P^{1/3} + A_T^{1/3})^2}, \quad (4)$$

where  $A_P$  and  $A_T$  are the projectile and target mass numbers. Using the above estimates, the factor  $\gamma_{P,T}$  is now written

$$\gamma_{P,T} = \frac{A_P}{\langle A_P^{\text{parti}} \rangle} \exp \left[ - \left[ \rho + \frac{A_P - A_T}{A_P + A_T} \right] \right], \quad (5)$$

where  $\rho$  is a normalization constant. Requiring that  $\gamma_{P,T} \rightarrow 1$  as  $A_P \rightarrow 1$  and  $A_T \rightarrow A_P$  (this requirement is specific to our choice to scale to proton-induced cross sections, scaling to other targets requires different normalizations) gives

$$\rho = \frac{A_P - 1}{A_P + 1}. \quad (6)$$

(Note that because of the fact that  $\langle A_P^{\text{parti}} \rangle$  has a finite variance associated with it,  $\rho$  will have a finite variance as well. However,  $\rho \approx 1$  for most collision systems and the variance is on the order of  $\pm 0.01$ .) The specific functional form for  $\gamma_{P,T}$  above can be shown (1) to approximate the various sum rules [10] concerning the conservation of baryon number and energy in the collision; (2) to repro-

duce the asymmetry between target and projectile (as we are interested in projectile fragments, being scattered by a heavy target is different from a lighter one for the same projectile nucleus, however, when accounting for all projectile as well as target fragments the symmetry between the projectile and target nuclei in the collision system is recovered); (3) to adhere to the participant-spectator picture; and (4) to reproduce the weak factorization property for projectile fragments.

The third prescription in this scaling algorithm is concerned with estimating the energy at which one uses the  $p$ -nucleus cross section to obtain the nucleus-nucleus cross section. To estimate this relevant excitation energy we develop the following criterion: Since only a fraction of the target nucleons actually do participate in fragmenting the projectile, we modulate the  $p$ -nucleus corresponding energy using  $\Psi(\langle A_T^{\text{parti}} \rangle)$ , i.e.,

$$E_{pN} = E_{NN} \Psi(\langle A_T^{\text{parti}} \rangle), \quad (7)$$

where  $E_{pN}$  is now the corresponding (scaled) total energy for calculating the  $p$ -nucleus cross section and  $E_{NN}$  is the energy per nucleon in the nucleus-nucleus collision. Realizing that  $\langle A_T^{\text{parti}} \rangle$  is only an impact-parameter-averaged quantity and the fact that spallation cross sections are sensitive functions of the impact parameter,  $\Psi(\langle A_T^{\text{parti}} \rangle)$  is now parametrized using the following prescription. *A priori* knowledge of the exact dependence of  $\Delta A (= A_p - A_f)$  on the impact parameter is not available,  $A_f$  being the mass number of the projectile fragment  $f$ . This dependence is essentially a detailed dynamical aspect of the collision system’s space-time evolution from entry channel (e.g., impact parameter) to final-state observables (e.g., fragments). Here, we make the assumption that when  $\Delta A \cong \langle A^{\text{parti}} \rangle$ ,  $\Psi(\langle A_T^{\text{parti}} \rangle) \rightarrow \langle A_f^{\text{parti}} \rangle$ ,  $\langle A^{\text{parti}} \rangle$  being the total (average) number of participants in the overlap volume  $\langle A_P^{\text{parti}} \rangle + \langle A_T^{\text{parti}} \rangle$ . In essence, this is not different from the simplifying assumption in relating the excitation energy of the projectile to the kinetic energy of the struck nucleons [7]. In the limit when  $\Delta A \ll \langle A^{\text{parti}} \rangle$ , i.e., spallation products, the number of struck target nucleons is expected to be much smaller than  $\langle A_T^{\text{parti}} \rangle$ . To parametrize this dependence, a simulated [11] impact-parameter-averaged relationship between  $\Psi$  and  $\Delta A$  is obtained which can be cast in the following functional form:

$$\Psi(\langle A_T^{\text{parti}} \rangle; \Delta A) \approx \langle A_T^{\text{parti}} \rangle \left[ 1 + \tanh \left[ \frac{\Delta A - \langle A^{\text{parti}} \rangle}{\langle A^{\text{parti}} \rangle} \right] \right], \quad (8)$$

where  $\Psi$  in Eq. (7) now takes the parametrized form of Eq. (8). The energy-modulating function above is intended for projectile fragments with  $A_f \leq A_P/2$  (i.e., spallation and deep-spallation products). However, the parametrization does extend (for normalization purposes) beyond this limit up to  $A_P$ . The parametrization  $\Psi(\langle A_T^{\text{parti}} \rangle; \Delta A)$  allows for the modulation to vary between the limits of  $\gtrsim 1$  and  $2 \langle A_T^{\text{parti}} \rangle$ .

### III. TESTING THE ALGORITHM

The above algorithm has been implemented numerically in such a way to take advantage (and supplement) the existing  $p$ -nucleus cross-section routines. To test the robustness of the algorithm we apply it to collision systems with varying degrees of asymmetry (between target and projectile) at different beam energies. To that end and due to the availability of data [12–18,21–22], we choose the fragmentation of  $^{56}\text{Fe}$ ,  $^{32}\text{S}$ ,  $^{16}\text{O}$ , and  $^{12}\text{C}$  by various targets from  $^{12}\text{C}$  to  $^{238}\text{U}$ . We use projectile-fragment data over the energy range 0.25–2.1 GeV/nucleon.

In Figs. 1 and 2 we show the partial cross sections for the production of the subiron group as  $^{56}\text{Fe}$  fragments for  $^{56}\text{Fe}$  kinetic energies from 0.1 to 2.0 GeV/nucleon. Data are from Refs. [12–15]. This cross section is defined as  $\sum_{z=21}^{25}\sigma(z)$ . On all the figures, the solid curves represent the calculated cross sections using the scaling algorithm (denoted  $A$ ). Short-dashed curves represent the simulated cross sections using FREESCO [11]. On the basis of 5000 simulated events, statistical fluctuations (not shown) are on the order of  $\pm 12\%$ . Long-dashed curves denoted by ST represent calculations using the semiempirical scaling procedure of Silberberg and Tsao [6]. Curves denoted SE represent calculations using our semiempirical scaling procedure [4]. Those denoted by LST represent calculations

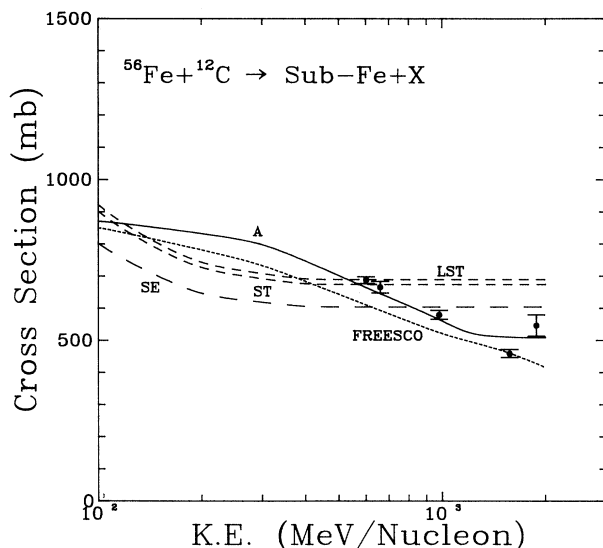


FIG. 1. Production of the subiron group,  $\sum_{z=21}^{25}\sigma(z)$ , from the fragmentation of  $^{56}\text{Fe}$  by  $^{12}\text{C}$  at energies 0.1–2.0 GeV/nucleon. Data are from Refs. [12–15]. On all the figures, the solid curves represent the calculated cross sections using the scaling algorithm (denoted  $A$ ). Long-dashed curves denoted by SE represent calculations using our earlier semiempirical procedure [4]. Short-dashed curves represent the simulated cross sections using FREESCO [11]. Statistical fluctuations (not shown) in the simulated cross sections are on the order of  $\pm 12\%$ . Long-dashed curves denoted by ST represent calculations using the semiempirical scaling procedure of Silberberg and Tsao [6], while those denoted by LST are due to Letaw, Silberberg, and Tsao [5].

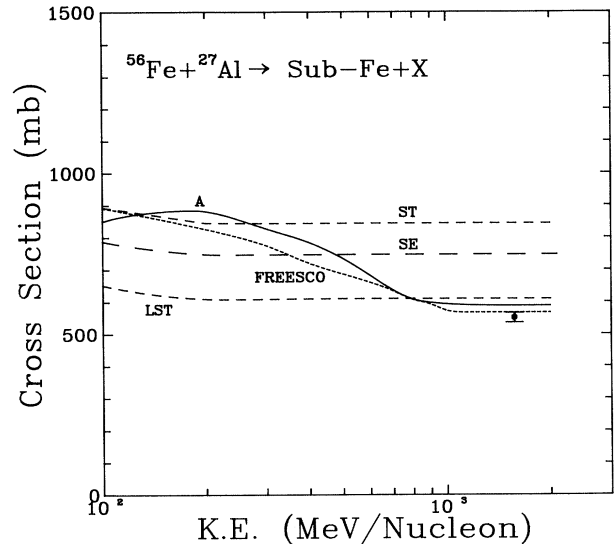


FIG. 2. Same as in Fig. 1 except the target here is  $^{27}\text{Al}$ .

using an earlier semiempirical scaling procedure due to Letaw, Silberberg, and Tsao [5] that has been used as part of the cosmic-ray propagation and spallation model UPROP [19]. ST and LST in Fig. 1 tend to flatten out beyond 0.5 GeV/nucleon. This is so because in both scaling procedures the energy at which the corresponding  $p$ -nucleus cross section is calculated is simply the nucleus-nucleus energy per nucleon multiplied by the mass number of the target nucleus. For  $^{12}\text{C}$  and realizing that  $p$ -nucleus cross sections as functions of beam energy tend to saturate at 2–3 GeV, the scaled  $p$ -nucleus cross sections are thus expected to saturate at such energies divided by the mass number of the target nucleus. In essence, both of these procedures predict insensitivity of the projectile-fragment cross section to the projectile kinetic energy except only for light targets. Both the simulated energy dependence and  $A$  appear to correspond very closely to each other as well as to the available high-energy data. In fragmentation of  $^{56}\text{Fe}$  by  $^{27}\text{Al}$  targets (Fig. 2), similar projectile-energy dependence in both the simulation and  $A$  is seen as in Fig. 1. Note, however, the behavior of ST and LST predictions: For heavy targets ST tends to approximate the low-energy behavior while LST the high-energy behavior. SE and ST appear to differ little in their overall predictions.

Figures 3 and 4 show the partial cross section for the production of Mn for collisions of  $^{56}\text{Fe}$  and  $^{12}\text{C}$  and  $^{27}\text{Al}$ , respectively. Data are from Refs. [12–15]. Here, too, the low-energy (ST) and high-energy (LST) approximations are evident. Also,  $A$  and FREESCO appear to approximate similar energy dependences. There is, however, a tendency in  $A$  to overestimate the yield for energies above 1 GeV/nucleon. The overestimation appears to stem from the fact that  $A$  calculations tend to saturate at lower energies than what the data suggest. In part, we attribute that to having to use averaged quantities for estimating the projectile and target participants, which, in turn, were used to calculate the cross sections as well as to scale the excitation energy [Eqs. (5) and (8)]. Manko

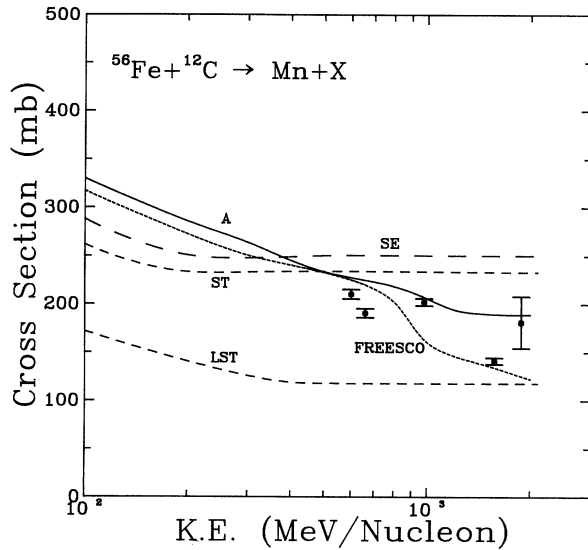


FIG. 3. Same as in Fig. 1 except the projectile fragment here is Mn.

and Nagamiya [20] have reported that these estimates based on Glauber scattering theory tend to be over-predicted for nearly equal-mass collisions. Nonetheless, the overall energy dependence seems to be well reproduced by A.

To compare the results of the algorithm to those from our earlier semiempirical procedure [4] we show in Fig. 5 the calculated partial elemental cross sections of  $^{12}\text{C}$  on  $^{12}\text{C}$  collisions at energies 0.1–2.0 GeV/nucleon. Data are from Refs. [7,12,21]. The energy-dependence behavior of A is clear whereas SE appears to better approximate the behavior at 600 MeV/nucleon and higher, even though both curves appear to correspond to the data with comparable accuracy on the average. Both A and SE incorporate semiempirically derived [4] enhance-

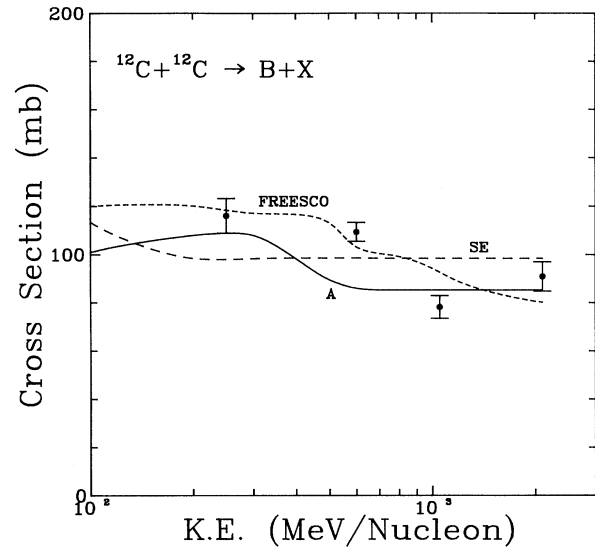


FIG. 5. Partial elemental production cross sections for B from  $^{12}\text{C}$  on  $^{12}\text{C}$  collisions at energies 0.1–2.0 GeV/nucleon. Data are from Refs. [7,12,21]. Note neither data nor calculations include the  $^9\text{B}$  isotope.

ment factors that are applicable to light fragments like B here.

In order to estimate the accuracy of the algorithm it becomes necessary to isolate the uncertainties (estimated at around 25%) due to the semiempirical  $pN$  cross-section predictions from those inherent in the scaling procedure. (Note that no light-fragment enhancement factors are involved here.) For that purpose and due to the availability of proton-induced spallation data (for  $^{56}\text{Fe}$  and  $^{16}\text{O}$ , for example) over the energy range of interest, we devise the following test. The scaled Mn and N (as examples of spallation products) cross sections (from  $NV$  collisions) are divided by the corresponding  $pN$  cross sections over the beam-energy range 0.1–2.0 GeV/nucleon for the same projectile at the same energy/nucleon, giving us the theoretically calculated scaling factors  $\gamma_{\text{the}}$ . These factors are then compared with the experimental, similarly deduced ones  $\gamma_{\text{expt}}$ . The results are in Tables I–III, which seem to suggest an overestimation in the calculated scaling factor for nearly equal-mass collisions. This is consistent with Figs. 3 and 4 as it clearly points to the energy scaling step in the procedure. Recall that this is the step [Eq. (8)] where any

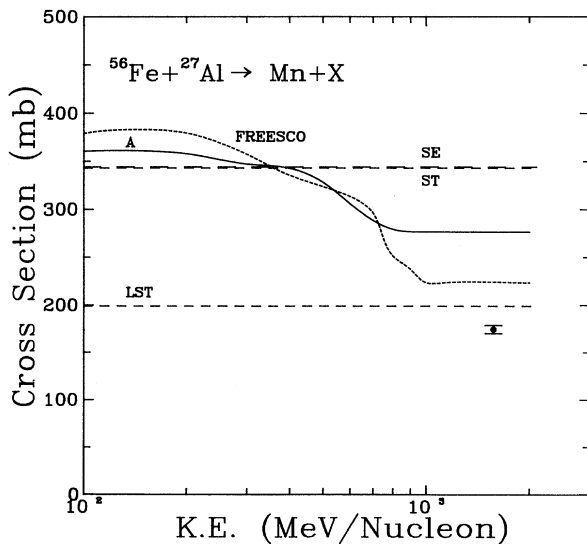


FIG. 4. Same as in Fig. 2 except the projectile fragment here is Mn.

TABLE I. Sample theoretical  $\gamma_{\text{the}}$  and experimental  $\gamma_{\text{expt}}$  scaling factors for the production of Mn from  $^{56}\text{Fe}$  at different energies.

$E_{\text{kin}}$ (GeV/nucleon)	Target	$\gamma_{\text{expt}}^a$	$\gamma_{\text{the}}$	$\gamma_{\text{the}}/\gamma_{\text{expt}}$
0.6	$^{12}\text{C}$	$1.54 \pm 0.06$	1.40	$0.91 \pm 0.06$
1.0	$^{12}\text{C}$	$1.76 \pm 0.07$	1.44	$0.82 \pm 0.07$
1.5	$^{12}\text{C}$	$1.39 \pm 0.06$	1.49	$1.07 \pm 0.06$
1.9	$^{12}\text{C}$	$1.43 \pm 0.24$	1.39	$0.97 \pm 0.24$
1.5	$^{27}\text{Al}$	$1.79 \pm 0.07$	2.18	$1.22 \pm 0.07$
1.9	$^{238}\text{U}$	$5.09 \pm 1.0$	5.91	$1.16 \pm 0.23$

<sup>a</sup>Data are from Refs. [12–16].

TABLE II. Sample theoretical  $\gamma_{\text{the}}$  and experimental  $\gamma_{\text{expt}}$  scaling factors for the production of N from  $^{16}\text{O}$  at different energies.

$E_{\text{kin}}$ (GeV/nucleon)	Target	$\gamma_{\text{expt}}^{\text{a}}$	$\gamma_{\text{the}}$	$\gamma_{\text{the}}/\gamma_{\text{expt}}$
0.6	$^{12}\text{C}$	$1.44 \pm 0.06$	1.37	$0.95 \pm 0.06$
0.9	$^{12}\text{C}$	$1.62 \pm 0.13$	1.53	$0.94 \pm 0.08$
2.1	$^{12}\text{C}$	$1.17 \pm 0.10$	1.41	$1.21 \pm 0.10$
2.1	$^{63}\text{Cu}$	$1.90 \pm 0.14$	2.05	$1.08 \pm 0.14$
0.9	$^{208}\text{Pb}$	$4.11 \pm 0.37$	3.81	$0.93 \pm 0.08$
2.1	$^{208}\text{Pb}$	$2.97 \pm 0.18$	2.89	$0.97 \pm 0.18$

<sup>a</sup>Data are from Refs. [7,12,17,18].

overestimation of  $\langle A_p^{\text{parti}} \rangle$  will overestimate the excitation energy forcing the energy dependence to saturate at a faster rate than what the data suggest. However, the calculated scaling factors are in good agreement with the experimental ones especially for asymmetric-mass systems at both low and high energies. (We have calculated the ratio [23] of  $\gamma_{\text{the}}$  to  $\gamma_{\text{expt}}$  for  $^4\text{He}$  targets. For energies below 1 GeV/nucleon and for light projectiles,  $^{12}\text{C}$  and  $^{16}\text{O}$ , the ratio is very close to one. However, the ratio appears to be consistently 0.5 higher than one for heavier projectiles over the energy range 0.6–2.0 GeV/nucleon. In the context of the above-described algorithm,  $^4\text{He}$  targets represent a special case for reasons related to the normalization criterion [Eq. (6)] in the limit of convergence to the  $p$ -nucleus limit. Realizing that  $^4\text{He}$  targets are also of special astrophysical interest, e.g., spallation of cosmic rays with interstellar helium, we are currently developing a scaling algorithm applicable to those situations.)

Based on the above test, the systematic uncertainty in the algorithm cross-section predictions is about 10–22 % with an average of 15% over the energy range considered. Note, in addition, that for energies below 1 GeV/nucleon the systematic uncertainty is better than 10% growing to 22% for energies above 1 GeV/nucleon. Finally, when comparing the calculated cross sections to the simulated ones as well as to data (this includes the semiempirical  $pN$  predictions) we find the same systematic uncertainties to hold true for both energy regimes (Figs. 1–4). This further points to the need to understand and improve upon the above-mentioned overestimation of the excitation energy (for nearly equal-mass collision systems) due to the overestimation of  $\langle A_p^{\text{parti}} \rangle$  and thus  $E_{pN}$ . We plan to formulate such an improvement by further studying the dependence of  $\Psi$  [Eq. (8)] on impact parameter using the simulation model FREESCO.

In light of the above two tests we feel that the scaling algorithm we have presented offers marked improvement over earlier semiempirical procedures. It is applicable for the prediction of projectile-fragment cross sections for projectile kinetic energies 0.1–2.0 GeV/nucleon with no

TABLE III. Sample theoretical  $\gamma_{\text{the}}$  and experimental  $\gamma_{\text{expt}}$  scaling factors for the production of Al from  $^{32}\text{S}$ .

$E_{\text{kin}}$ (GeV/nucleon)	Target	$\gamma_{\text{expt}}^{\text{a}}$	$\gamma_{\text{the}}$	$\gamma_{\text{the}}/\gamma_{\text{expt}}$
0.7	$^{12}\text{C}$	$1.47 \pm 0.11$	1.32	$0.90 \pm 0.10$
0.7	$^{108}\text{Ag}$	$2.32 \pm 0.26$	1.88	$0.81 \pm 0.10$

<sup>a</sup>Data are from Ref. [22].

restrictions on the asymmetry nor the size of the collision system apart from the special case of  $^4\text{He}$  as a target.

#### IV. SUMMARY AND CONCLUDING REMARKS

We have presented an algorithm to scale heavy-ion-induced projectile-fragment cross sections from the corresponding proton-induced ones. The algorithm relies on the weak factorization property of projectile fragments. The other two features of the algorithm are the taking into account of the asymmetry between target and projectile sizes in a consistent fashion and the scaling of the  $p$ -nucleus energy in adherence with the participant-spectator model of high-energy nucleus-nucleus collisions as well as using Glauber scattering theory. The only normalizations used are those to approximate sum rules and convergence to the  $p$ -nucleus limit. (Some semiempirically derived [4] enhancement factors are still used, however, for the lightest collision products.)

The algorithm is sufficiently robust over the energy range 0.1–2.0 GeV/nucleon with no restrictions on the sizes of target nor projectile nuclei. (The special case of  $^4\text{He}$  targets is currently under study.) It offers marked improvement over earlier semiempirical scaling procedures which tend to either approximate the high-energy or the low-energy behavior but not both in a consistent fashion. Using measured and simulated cross sections for comparison, estimated systematic uncertainty of the algorithm over this energy range is better than 10% for energies below 1 GeV/nucleon and about 20% for higher energies, averaging  $\sim 15\%$ . Although some improvement regarding the energy-scaling step in the procedure may be added for even better correspondence to data, the algorithm does promise to be an efficient and sufficiently accurate tool for modeling and analysis of cosmic rays and other nuclear spallation data.

#### ACKNOWLEDGMENTS

A.F.B.'s summer appointment at NRL has been supported by the Navy-ASEE 1992 Summer Faculty Research Program. A.F.B. gratefully acknowledges the strong support and valuable insights of Dr. J. H. Adams, Jr. and Dr. A. J. Tylka of the Cosmic Ray Section–E.O. Hulburt Center for Space Research, Naval Research Laboratory. L.S. gratefully acknowledges the support of the STA (Japan) Fellowship Program. This work was supported by ONR.

[1] J. H. Adams, Jr., Nucl. Tracks Rad. Meas. **20**, 397 (1992).  
 [2] J. R. Letaw, R. Silberberg, and C. H. Tsao, in *Terrestrial Space Radiation and Its Biological Effects*, edited by P. D.

McCormick, C. E. Swenberg, and H. Bückner (Plenum, New York, 1988), p. 663.

[3] R. Silberberg and C. H. Tsao, in *Proceedings of the 21st In-*

- ternational Cosmic Ray Conference, Adelaide, Australia*, edited by R. J. Protheroe (The University of Adelaide Press, Adelaide, Australia, 1990), Vol. 3, p. 424.
- [4] L. Sihver, C. H. Tsao, R. Silberberg, T. Kanai, and A. F. Barghouty, *Phys. Rev. C* **47**, 1225 (1993); L. Sihver and T. Kanai, Report No. NIRS (Japan)-M-87, 1992; Report No. HIMAC-002, 1992.
- [5] J. R. Letaw, R. Silberberg, and C. H. Tsao, *Astrophys. J. Suppl.* **51**, 271 (1984).
- [6] R. Silberberg and C. H. Tsao, *Phys. Rep.* **191**, 351 (1990).
- [7] D. L. Olson, B. B. Berman, D. E. Greiner, H. H. Heckman, P. J. Lindstrom, and H. J. Crawford, *Phys. Rev. C* **28**, 1602 (1983).
- [8] For a review of this see, e.g., H. Hüfner, *Phys. Rep.* **125**, 129 (1985), and references therein.
- [9] R. J. Glauber and G. Matthiae, *Nucl. Phys.* **B21**, 135 (1970); J. Hüfner and J. Knoll, *ibid.* **A290**, 460 (1977); for a description of the collision geometry see, e.g., S. Nagamiya and M. Gyulassy, *Adv. Nucl. Phys.* **13**, 201 (1984), and references therein.
- [10] X. Campi, J. Desbois, and E. Lipparini, *Phys. Lett.* **138B**, 353 (1984).
- [11] For a description of the latest version of the simulation model used, see A. F. Barghouty, G. Fai, and D. Keane, *Nucl. Phys.* **A535**, 715 (1991), and references therein.
- [12] W. R. Webber, J. C. Kish, and D. A. Schrier, *Phys. Rev. C* **41**, 547 (1990).
- [13] W. R. Webber and D. A. Brautigam, *Astrophys. J.* **260**, 894 (1982).
- [14] J. R. Cummings, T. L. Garrard, M. H. Israel, J. Klarman, E. C. Stone, C. J. Waddington, W. R. Binns, *Phys. Rev. C* **42**, 2508 (1990).
- [15] G. D. Westfall, L. W. Wilson, P. J. Lindstrom, H. J. Crawford, D. E. Greiner, and H. H. Heckman, *Phys. Rev. C* **19**, 1309 (1979).
- [16] C. Perron, *Phys. Rev. C* **14**, 1108 (1976).
- [17] P. J. Lindstrom, G. E. Greiner, H. H. Heckman, B. Cork, and F. S. Bieser, LBL Report 3650, 1975.
- [18] S. E. Hirzebruch, W. Heinrich, K. D. Tolstov, A. D. Kovalenko, and E. V. Benton, *Phys. Rev. C* **46**, 1487 (1992).
- [19] UPROP, A Heavy-Ion Propagation Code, SCC Report 89-02, Severn Commun. Corp., Millersville, MD, 1989.
- [20] V. I. Manko and S. Nagamiya, *Nucl. Phys.* **A384**, 475 (1982).
- [21] J. M. Kidd, P. J. Lindstrom, H. J. Crawford, and G. Woods, *Phys. Rev. C* **37**, 2613 (1988).
- [22] C. Brechtmann and W. Heinrich, *Z. Phys. A* **331**, 463 (1988).
- [23] P. Ferrando, W. R. Webber, P. Goret, J. C. Kish, D. A. H. Schrier, A. Soutoul, and O. Testard, *Phys. Rev. C* **37**, 1490 (1988).